International Journal of Automotive Technology, Vol. 21, No. 5, pp. 1247−1256 (2020)
DOI 10.1007/s12239−020−0118−4

pISSN 1229−9138/ eISSN 1976−3832

ONLINE OPTIMAL CONTROL STRATEGY METHODOLOGY FOR POWER-SPLIT HYBRID ELECTRIC BUS BASED ON HISTORICAL DATA

Xiaohua Zeng, Zhenwei Wang, Yue Wang* and Dafeng Song

State Key Laboratory of Automotive Simulation and Control, Jilin University, Changchun 130025, China

(Received 6 September 2019; Revised 26 December 2019; Accepted 26 December 2019)

ABSTRACT−An online optimal control strategy methodology on the basis of historical data for a power-split hybrid electric bus (HEB) is proposed in this study. This approach aims to fully utilize the fuel-saving capability of power-split HEB under real operating cycles and provide an effective way for solving the optimal calibration problem in the application promotion. Firstly, a procedure for synthesizing real-world driving cycles based on cluster analysis and Markov chain method is constructed. Subsequently, dynamic programming (DP) control algorithm is performed to explore the fuel economy potential. Moreover, a DP-based rule control strategy with an automated implementation foundation is introduced to achieve online approximate optimal effect. Finally, offline simulation and hardware-in-the-loop test are conducted. Simulation results validate that the proposed online optimal control strategy methodology has similar fuel-saving performance to DP optimal results and good real-time application conditions.

KEY WORDS : Power-split hybrid electric bus, Online optimal control strategy methodology, Driving cycle synthesis, Fuel economy potential, Hardware-in-the-loop (HIL)

NOMENCLATURE

θ_t : feature vector of synthesized cycle
θ_i : feature vector of historical data
x : state vector
u : control variable
L : instantaneous cost
SOC_{min} : allowable lower limit of SOC range, %
SOC_{max} : allowable upper limit of SOC range, %
$P_{bat,min}$: allowable lower limit of battery power, kW
$P_{bat,max}$: allowable upper limit of battery power, kW
$d(p,o)$: distance between two working points p and o
$d_k(p)$: kth distance far away from operating point p
$N_k(p)$: kth distance neighborhood for point p
$reach\text{-}dist_k(p,o)$: kth reachable distance between points o and p
Lrd : local reachable density
$N_{kk}(p)$: inverse kth distance neighborhood for point p
$NN_k(p)$: union of set $N_k(p)$ and set $N_{kk}(p)$
$NLOF(p)$: new density-based local outlier factor for point p

1. INTRODUCTION

With the increasing concern toward energy shortage and environmental pollution, hybrid technology has become an important branch of automotive technology and industrial innovation (Awadallah *et al*., 2017; Gavgani *et al*., 2016). The city bus is an important part of public transportation; hence, the development of hybrid buses is of great importance for improving energy consumption and urban environment. With the potential for achieving high fuel economy, power-split hybrid electric vehicles (HEVs) have been seen as a hybrid powertrain architecture to improve fuel economy (Zeng *et al*., 2016; Wang *et al*., 2014; Qi et *al*., 2018). The application of power-split systems to public transport of urban areas has become an important trend in the automotive industry. With the decline of policy subsidies, power-split systems have become an important product layout for automotive companies to achieve strategic transformation.

The fuel economy of power-split systems is highly correlated with driving cycles. Thus far, certification driving cycles are primary choices for vehicle design because of their use by legislative authorities for fuel economy and emission certification (Chen *et al*., 2017; Borthakur and Subramanian, 2018; Mangun *et al*., 2017; Fu *et al*., 2017; Gujarathi *et al*., 2017). However, vehicle operating conditions have discrepancies in different regions, road characteristics, time, and even climatic conditions. The paper of Shahidinejad *et al.* (2010) stated that many problems exist in driving cycles, such as the underestimation of cruise, acceleration, and stop-and-go activities in different velocity brackets. They concluded that the real-world power demands of vehicles are difficult to completely emulate by existing certification cycles. At present, calibration engineers usually need to perform a large number of calibration work, which greatly increases

**Corresponding author*. e-mail: wang_yue16@mails.jlu.edu.cn

the system promotion cost, to ensure fuel economy in a specific driving cycle. In addition, the calibration effect depends on the experience of calibration engineers, wherein consistency and optimality of calibration results are often difficult to ensure (Duan *et al.*, 2017).

Present hybrid electric buses (HEBs) usually have remote data monitoring equipment that can collect critical operation data from vehicles. Effective use of historical operation data can provide guidance and assistance for system optimization; it is also an important exploration for the use of big data. Therefore, exploring a new driving cycle synthesis method to characterize the vehicle operating operation is an important basis to ensure that an optimal control strategy can be applied to specific application scenarios. The method will effectively reduce the large calibration workload of current power-split buses and improve the fuel economy under real operating cycles. Huertas *et al*. (2018) developed a methodology to obtain representative driving cycles based on simultaneous data of speed, altitude, fuel consumption and tail pipe emissions. Zhao *et al*. (2018) created the comprehensive principal component score to cluster micro-trips into homogeneous groups of observations; this method has good robustness. Peng *et al*. (2019) applied principal component analysis and K-means clustering method to establish a representative driving cycle for public urban buses in Fuzhou City. Lee *et al.* (2011) synthesized representative naturalistic cycles through a stochastic process utilizing transition probability matrices extracted from naturalistic driving data collected in the Midwest region of the United States.

The power-split system includes multiple power sources with complex nonlinear efficiency characteristics. The fuel-saving effects in different application scenarios are dependent on control strategies. At present, the dynamic programming (DP) algorithm has been demonstrated effective in finding the best fuel economy over certain drive cycles (Xi *et al.*, 2016; Dong *et al.*, 2014; Yang *et al.*, 2014; Xi *et al.*, 2018). However, given that realizing DP algorithm in practice is difficult, rule-based control based on DP algorithm has been widely used. Kum *et al.* (2011) adopted a comprehensive rule extraction method to extract the mode switching rules, shift rules, and optimized power split ratio by observing the DP results of a plug-in hybrid system. Zhang *et al.* (2014) applied rule-based control as an implementable controller with DP results on the basis of the position and battery SOC. Peng *et al*. (2016) proposed a recalibration method to improve the performance of a rule-based control strategy through the results calculated by DP algorithm. Biasini *et al.* (2013) utilized DP algorithm to minimize fuel consumption over a given driving mission. The near-optimal rules were extracted and tuned to design a rule-based strategy for charge-sustaining operation through the analysis of DP control actions.

However, current rule extraction methods are often an observation-based feedback correction process and rely on the experience of researchers. The change of driving conditions or vehicle parameters and component performance parameters may cause changes in global optimization results. Thus, ensuring universal adaptability in various driving cycles is difficult, that is, the method does not have the basis for automated implementation. To solve these limitations, an automatic control rule extraction method should be developed. Such a method can improve the robustness of online optimal control strategy to driving cycles, effectively reduce calibration time, and ensure the consistency of optimal effects.

This study attempts to explore a methodology to develop an online optimal control strategy with good application conditions and automatic implementation capability through the exploration of historical data. This methodology ensures that the system can maximize the fuel saving capability under different driving cycles and that the huge calibration workload. First, typical driving cycles are synthesized based on historical operation data. The synthesized driving cycle satisfies the probability distribution characteristics of the real operation condition. Thus, the control robustness of the optimal control strategy under specific operating conditions can be guaranteed. Subsequently, a global optimization solution is performed based on the synthesized cycle, and a novel control rule extraction method to achieve optimal effect similar to DP algorithm is proposed. In comparison with the existing methods, the new rule extraction method has a general application form, which is more helpful for engineers to understand and apply the control rules. Finally, the proposed online optimal control strategy is tested and validated through MATLAB/Simulink software and hardware-in-loop (HIL) simulation experiments.

The contributions of this study are as follows. (1) This study covers the complete design and development process of online optimal control strategy from cycle synthesis and global optimization to control rule extraction. It provides an effective way to solve optimal calibration problems in application promotion for power-split HEB systems. It also fully utilizes the fuel-saving capability under real operating cycles. (2) This study creates important conditions for the automation implementation of cycle synthesis, global optimization, and control rule extraction by using reasonable mathematical methods and indicators. Thus, this study can be an important part of big data computing platform in the future, which will create the possibility of online automatic calibration of vehicle control strategy.

The rest of this paper is organized as follows. Following the introduction, Section 2 describes the power-split system configuration. Section 3 presents the typical driving cycle synthesis based on historical operation data. The DP-based rule control strategy (RCS, DP-RCS) is presented and implemented in Section 4. Section 5 validates the online optimal control strategy under the synthesized cycle. Section 6 presents the conclusion of the study.

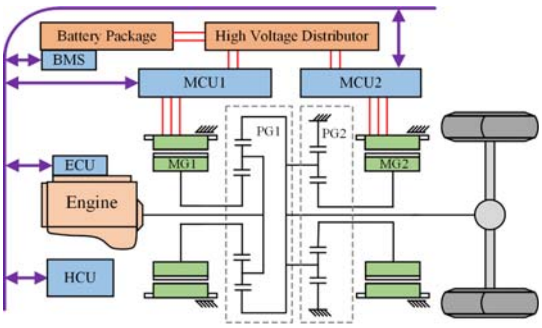

Figure 1. Configuration diagram of power-split HEB system.

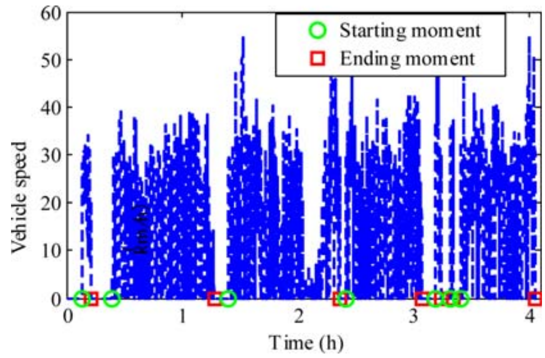

Figure 2. Screening of starting and ending moments.

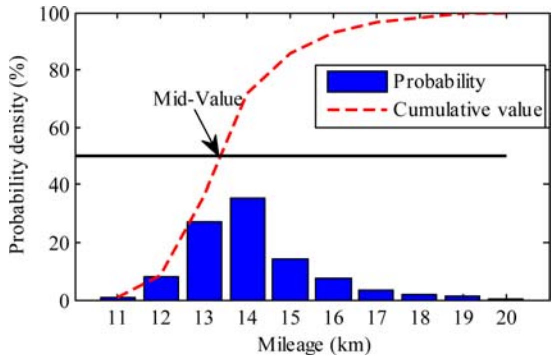

Figure 3. Probability density of mileage.

2. POWER-SPLIT HEB SYSTEM

The structure of the power-split HEB is shown in Figure 1. The main parts of the hybrid powertrain system include an engine, two PG sets, two motor/generator (M/G) sets, and a battery package. The PG1 set is the power-split device, and the PG2 set is the reducer given its fixed ring gear. The engine output shaft is connected to the carrier of PG1. MG1 is connected to the front sun gear, whereas MG2 is connected to the rear sun gear. The ring gear of PG1 is connected to the carrier of PG2, which is connected to the final drive. The battery package is used as the electric energy storage.

3. DRIVING CYCLE SYNTHESIS

This study focuses on developing an online optimal control strategy methodology based on the historical data of a real vehicle and expects to achieve optimal fuel economy of power-split HEB in different application scenarios. Therefore, typical driving conditions are synthesized and the statistical and probability distribution characteristics of driving conditions are effectively simulated to ensure that the control strategy can be applied to specific application scenarios.

3.1. Historical Data Analysis

Before the synthesis of real-world driving cycles, the constraint condition must be obtained by analyzing the historical operation data of real vehicles. For a power-split HEB, the distance of one round trip should be relatively close, and the driving time may vary significantly with traffic congestion. Therefore, distance is selected as the constraint condition for the synthesis of driving cycles. Given that each power-split HEB will wait for a long time at the terminal station, the Chauvenet method is applied to distinguish the starting and ending moments of vehicle operation data, as shown in Figure 2. The screening method has a comparatively large probability in finding the starting and ending moments of each cycle.

The distribution probability of the mileage obtained by Chauvenet method is shown in Figure 3. The probability shows an approximately normal distribution, with a specific mid-value of 13.4 km. Moreover, the statistical characteristics of vehicle operation data can be used as the test standard for the synthesis of driving cycles. Linear regression analysis was used to determine nine significant statistical indicators that can represent the cycle characteristic. The specific statistical indicator results are shown in Table 1.

3.2. Driving Cycle Synthesis Process

Clustering analysis and Markov methods are applied in the synthesis of driving cycles to ensure the representativeness and reduce the data processing pressure. The overall flowchart is shown in Figure 4. First, clustering analysis method is performed to classify kinematic fragments and calculate state transition probability matrix between each classification. Then, Markov method is applied to realize the random reorganization of kinematic fragments. When the reconstructed segment reaches the mileage boundary (13.4 km), the synthesis of single cycle ends. If the error between the feature vector of synthesized cycle θ_t and historical data θ_i is less than 5 %, then it is recorded as an option and the synthesis process is continued until the convergence condition is reached. Finally, the speed acceleration probability distribution (SAPD) and sum of SAPD squared difference (SSD) of all synthesized cycles

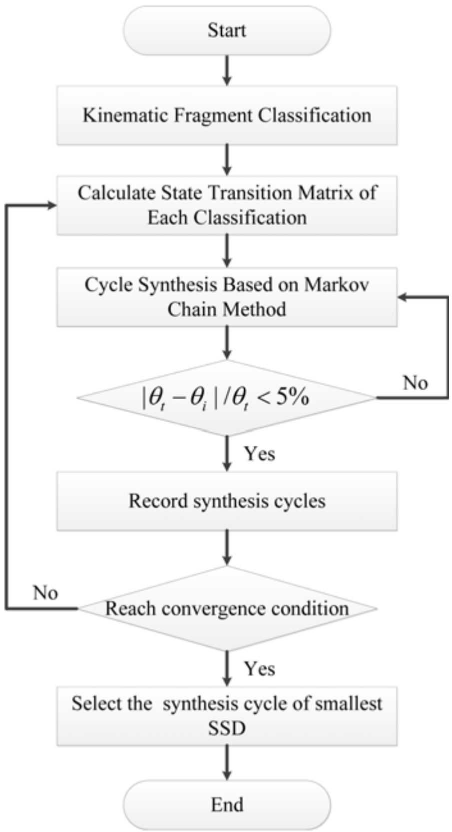

Figure 4. Flowchart of driving cycle synthesis.

are calculated. The candidate cycle with minimum SSD is taken as the most representative one.

Figure 5 show different classification quantities and SSD results under numerous iterations to determine the best classification number and convergence conditions. When the iteration number is sufficiently large, different classification quantities are nearly the same, and the overall SSD results show an approximate normal distribution. The classification number does not affect the cycle synthesis quality under a sufficient number of observations. Thus, from the perspective of understanding for engineers, the best classification number is 5. Meanwhile, the minimum SSD should be less than 3, which can be used as the convergence condition.

Taking the historical operating data of a power-split HEB on the same line as input, the aforementioned method is applied to complete the cycle synthesis process, and the result is shown in Figure 6. The process takes approximately 50 s, and the SSD of synthesized cycle is 2.63.

3.3. Evaluation and Validation of Synthesized Cycle

The statistical characteristics of real and synthesized cycles are compared to verify the rationality of the proposed method, as shown in Table 1. The results confirm that the proposed synthesis method can capture main features of

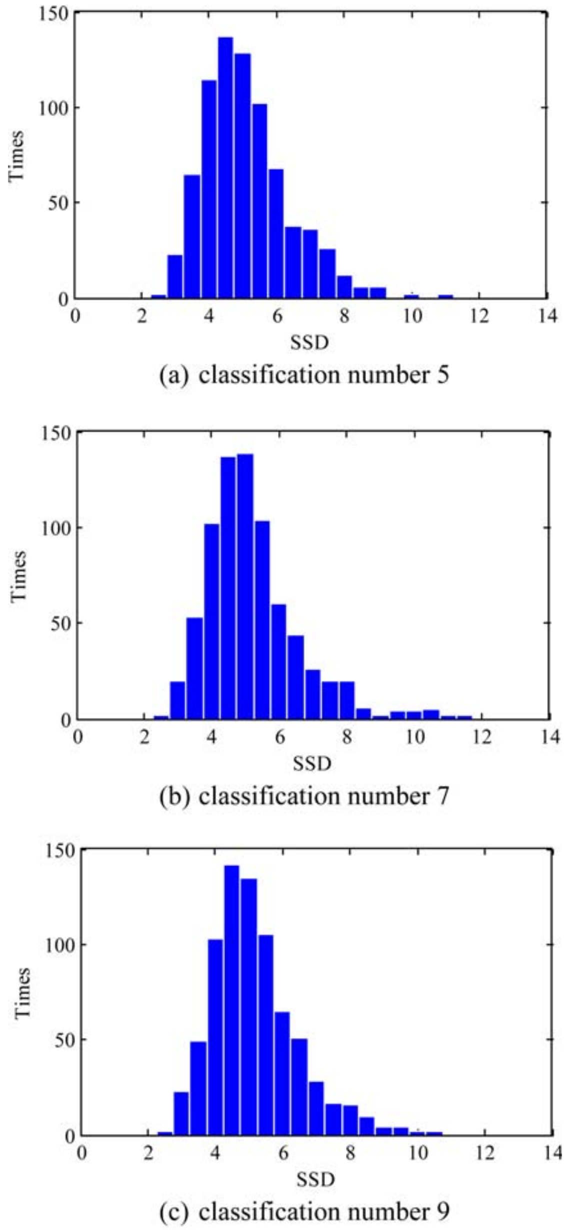

Figure 5. SSD results under numerous iterations.

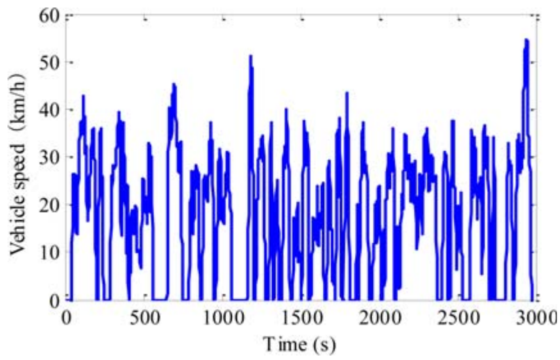

Figure 6. Synthesis result of driving cycle.

Table 1. Comparison of statistical characteristics.

Statistical characteristics	Real cycles	Synthesized cycle
Mean velocity: include zero velocity	17.6 km/h	17.3 km/h
Mean positive velocity	21.6 km/h	21.2 km/h
Standard deviation of velocity	11.1 km/h	11.4 km/h
Maximum velocity	56.0 km/h	55.0 km/h
Mean positive acceleration	0.35 m/s^2	0.35 m/s^2
Mean negative acceleration	− 0.43 m/s^2	− 0.43 m/s^2

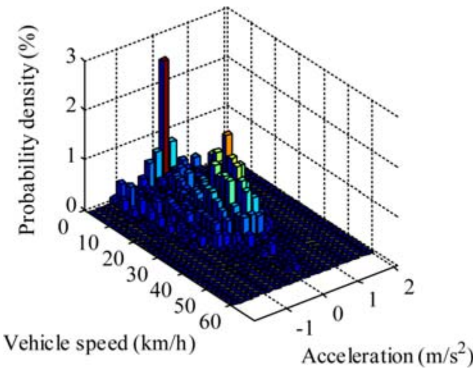

Figure 7. SAPD of real operation data.

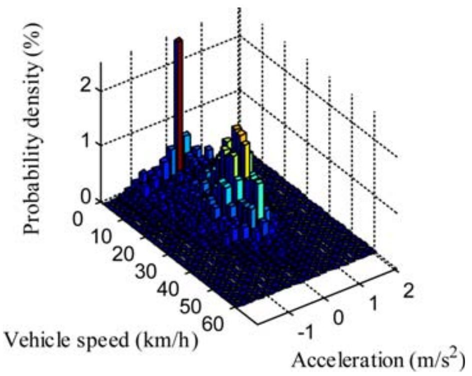

Figure 8. SAPD of synthesized cycle.

real-world driving conditions.

Any point of a cycle can be characterized by speed and acceleration; thus, the SAPD is a precise expression for various working conditions. The comparison result between the synthesized cycle and real operation data is shown in Figure 7 and Figure 8. The two SAPD distributions are similar. In summary, by comparing the statistical indicators and SAPD results, the synthesized cycle can well represent the original operation conditions of the power-split HEB.

4. DP-RCS

Synthesized cycle can effectively represent the statistical characteristics of historical driving conditions of real vehicles. In this section, a DP optimization problem is formed and solved, which guarantees a globally optimal solution in the synthesized cycle. The global optimization results are regarded as a reference and propose a novel extraction method of control rules based on DP results to formulate control strategies of real vehicles.

4.1. DP Control Algorithm

The DP method is an effective optimization algorithm for solving multistage decision problems. On the basis of Bellman optimization principle, the multistage decision problem is transformed into a series of single-stage problems. This approach simplifies the solution form of the optimization problem. The cost function is the minimum fuel consumption for a given HEV model on synthesized driving cycle, as shown as follows:

$$\begin{cases} \min\limits_{u(t)} J(u(t)) \\ J(u(t)) = G(x(t_f)) + \int_0^{t_f} L(x(t), u(t), t)dt \end{cases} \tag{1}$$

where $x(t)$ denotes the state vector (state of charge), $u(t)$ denotes the control variable (battery power P_{bat}), $L(x(t), u(t), t)$ is the instantaneous cost at each moment, $G(x(t_f))$ is penalty function based on the termination state, and t_f is the duration of the driving cycle.

During the optimization process, the following inequality constraints are necessary:

$$\begin{cases} P_{bat}(k) \in \left[P_{bat,min}, P_{bat,max}\right] \\ SOC(k) \in \left[SOC_{min}, SOC_{max}\right] \end{cases} \tag{2}$$

where SOC_{min} and SOC_{max} denote the lower and upper bounds of battery SOC, respectively; $P_{bat,min}$ and $P_{bat,max}$ denote the lower and upper bounds of battery power, respectively.

The iterative process of dynamic programming is shown in Figure 9. The minimum cost function of N-th step is:

$$J_N(x^i) = l_N(x^i) + g_N(x^i) \tag{3}$$

Then the minimum cost function in the (0 ~ N-th) step is:

$$J_k(x^i) = \min_{u_k \in [u_{min}, u_{max}]} \left\{ l_k(x^i, u_k) + g_k(x^i) + J_{k+1}(F_k(x^i, u_k)) \right\} \tag{4}$$

where x^i is ith variable in the discrete state variable grid, superscript i is dependent on the grid dimension, $l_k(x^i, u_k)$ is the instantaneous cost, $g_k(x^i)$ is the penalty function based on the current state x^i, and $J_k(x^i)$ is the cost function.

Minimum cost and optimal control variables at each moment can be calculated on the basis of the backward iterative process. According to the correspondence between the state and optimal control variables at each

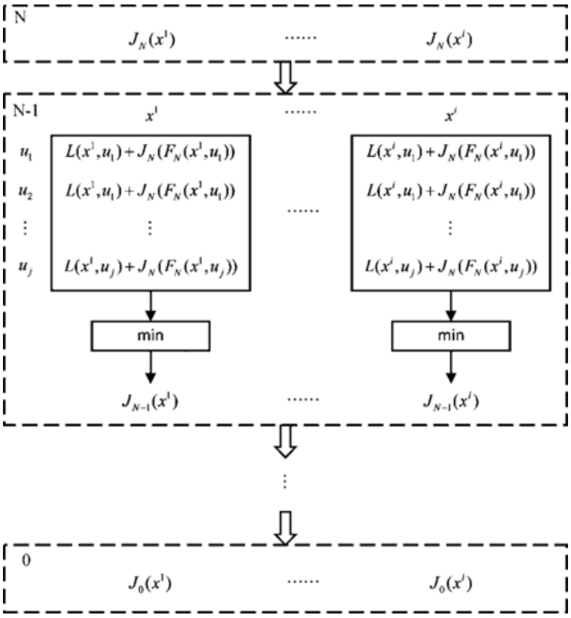

Figure 9. Iterative process of DP.

time, the optimal control path can be determined by the forward calculation based on a certain initial state variable.

4.2. Control Rule Extraction Based on DP Results

Despite guaranteed optimality of the DP solution, it has a long offline calculation time and cannot be directly implemented in the control of real vehicles, which need extraction method to obtain control rules. Conventional extraction methods often rely on the observation of researchers, which is not conducive to the application of optimization control rules. Thus, a new extraction method is proposed for the design of a DP-based control strategy. Figure 10 shows the optimal mode distribution result of DP algorithm. On the basis of the engine state, the power-split system can be divided into pure electric mode and hybrid mode. The former is mainly distributed in low-speed, small-demand torque range, whereas the latter is mainly distributed in high-speed, large-demand torque range. The two modes show a certain distribution trend but they also overlap in some intervals.

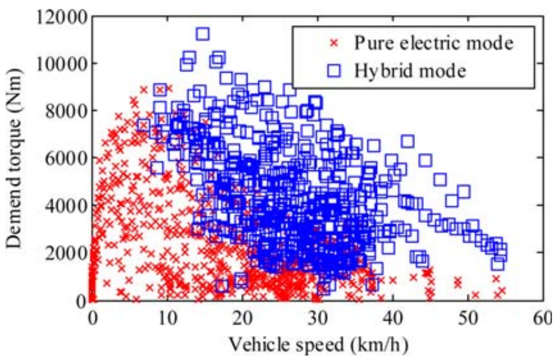

Figure 10. Optimal mode distribution result.

The rule extraction of mode switching analyzes the group characteristics of the system operating points in the same mode. The individual work points away from the group should be removed to obtain the analysis results of group feature, that is, the outlier detection method should be performed. First, the following key parameters of the method are defined.

(1) Distance between two working points p and o: $d(p,o)$;
(2) kth distance far away from operating point p: $d_k(p)$;
(3) kth distance neighborhood for point p: $N_k(p)$.

On the basis of the preceding definition, the kth reachable distance $reach\text{-}dist_k(p,o)$ between points p and o is shown in Equation (5); this distance is the one with the larger value between the kth distance far away from operating point o and the distance between two working points p and o :

$$reach\text{-}dist_k(p,o) = \max\{d_k(o), d(p,o)\} \tag{5}$$

On the basis of the reachable distance, the local reachable density of point p is expressed as:

$$Lrd_k(p) = 1 / \left[\frac{\sum_{o\in N_{k(p)}} reach\text{-}dist_k(p,o)}{|N_k(p)|} \right] \tag{6}$$

The local reachable density of point p indicates the reciprocal of $N_k(p)$ and average reachable distance $\sum_{o\in N_{k(p)}} reach\text{-}dist_k(p,o)$. The higher the value of the local reachable density is, the higher the probability that point p belongs to the same cluster as the surrounding neighborhood points; otherwise, the higher the probability that point p is an outlier.

Given that reverse neighbors are not considered, the outlier degree of data points is easily misjudged under certain data distribution conditions in the process of obtaining outliers in traditional algorithm. Therefore, a "friendly relationship" model is introduced to analyze the effect of reverse neighbors on the outliers of data points. The inverse kth distance neighborhood for point p is expressed as

$$N_{kk}(p) = \{o \mid o \in C, p \in N_k(o)\} \tag{7}$$

Where C is the data set.

Therefore, the new density-based local outlier factor $NLOF$ for each data point is calculated as

$$NN_k(p) = N_k(p) \cup N_{kk}(p) \tag{8}$$

$$Lrd(NN_k(p)) = \frac{\Sigma_{o\in NN_k(p)} Lrd_k(o)}{|NN_k(p)|} \tag{9}$$

$$NLOF(p) = \frac{Lrd_k(NN_k(p))}{Lrd_k(p)} \tag{10}$$

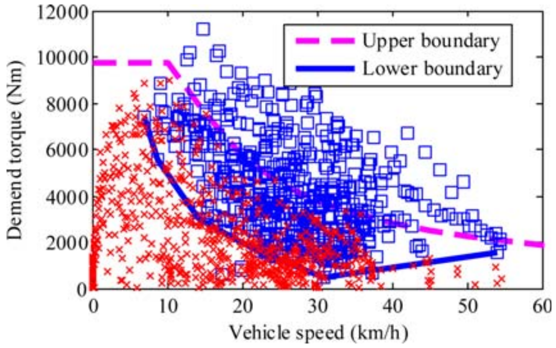

Figure 11. Rule extraction result of mode switching.

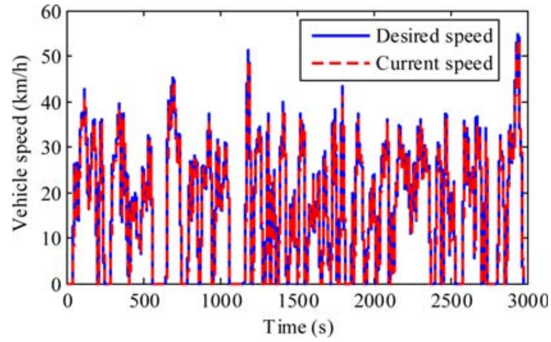

Figure 12. Vehicle speed in simulation.

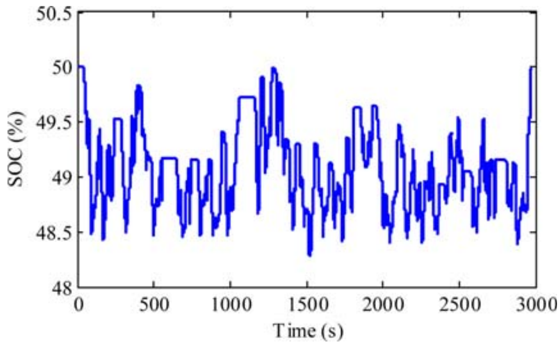

Figure 13. SOC in simulation.

The larger the value of *NLOF* is, the lower the density of *p* and is smaller than the average density of the points in its neighborhood, which indicates that it may be an outlier. Otherwise, the smaller the value of *NLOF* is, the lower the density of *p* but larger than the average density of the points in its neighborhood, which indicates that it is a normal point. When the value of *NLOF* is close to 1, *p* is equivalent to the density of points in the neighborhood, which belongs to the same cluster.

After eliminating the aforementioned outliers, convex envelope algorithm (Wang *et al*., 2015) can be used to obtain outer envelope points of the remaining working points. The lower boundary of the hybrid mode and the upper boundary of the pure electric mode are finally determined, as shown in Figure 11. When the demand torque at current velocity is less than the lower boundary, the system operates in pure electric mode. When the demand torque is greater than the upper boundary of pure electric mode, the system operates in hybrid mode.

By extracting the control rules of the algorithm and extending it to the original OOL RCS (OOL-RCS), the fuel economy can be further improved and directly applied to the control of real vehicles.

5. SIMULATION AND ANALYSIS

5.1. Offline Simulation

The simulation model of the power-split HEB system based on synthesized cycle is established on MATLAB/Simulink platform to validate DP-RCS. The parameters of the power-split HEB system are shown in Table 1. In the simulation the HEB speed follows the cycle well, and the SOC stays balanced, as shown in Figure 12 and Figure 13.

Subsequently, the operating points of engine under the DP algorithm and DP-RCS are shown in Figure 14. The distributions of engine operating points under two strategies are generally consistent, which verify the approximate optimal control effect of DP-RCS.

Fuel economy is the most concentrated indicator of power-split HEB system. The improvement of fuel economy can be used to validate the optimal effect of DP-RCS. The OOL-RCS commonly used in engineering, DP algorithm, and DP-RCS are selected to compare the fuel economy. The comparison results are shown in Table 2. The terminated battery SOC of all strategies under synthesized cycle are close to 50 %. Under this condition, in comparison with OOL-RCS, DP algorithm can obtain the best fuel economy, and the fuel consumption per 100 km is decreased by 9.0 %. The fuel consumption per 100 km of DP-RCS is decreased by 7.0 %, which is close to the results of DP algorithm.

5.2. HIL Simulation

A HIL experiment is performed to evaluate the real-time performance of DP-RCS. Figure 15 shows a photo of the HIL experiment bench is shown in, which mainly includes

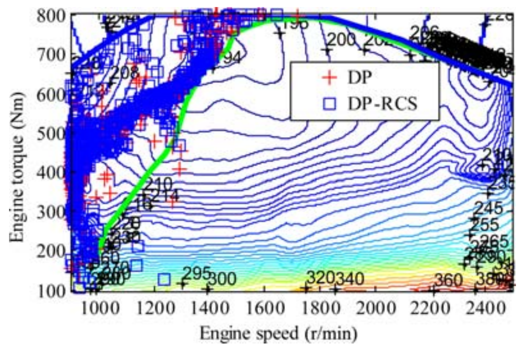

Figure 14. Comparison of engine operating points.

Table 2. Fuel economy of various control algorithms.

Control algorithm	Initial/ terminated SOC (%)	Fuel consumption (L/100 km)	Ratio of fuel saving (%)
OOL-RCS	50.00/49.95	19.81	-
DP	50.00/50.00	18.02	9.0
DP-RCS	50.00/49.96	18.43	7.0

the dSPACE simulator, vehicle control unit (VCU), low-voltage power supply (LVPS), and monitoring device. The dSPACE simulator is the real-time simulation platform. The LVPS supplies 24 volt DC voltage for the VCU. The VCU mainly communicates with the dSPACE simulator via CAN bus. The vehicle and driver models are integrated and uploaded to the dSPACE simulator, whereas the control strategy is uploaded to the VCU.

Figure 16 and Figure 17 show the velocity and SOC simulation results of DP-RCS based on synthesized cycle are shown in. On the basis of the communication protocol, the resolution of the battery SOC signal is set to 0.4 %. Therefore, the SOC signal acquired from the CAN bus exhibits a stepwise change. The simulation results show that the velocity follows the synthesized cycle well, and the SOC maintains balance.

The fuel consumption of power-split HEB under synthesized cycle is 18.81 L/100 km. The fuel consumption of DP-RCS is slightly deviated from the offline simulation result but is generally close to the offline simulation result. This finding is due to the signal accuracy and response delay caused by real-time transmission and implies that the DP-RCS can obtain approximate optimal control effect under real-time conditions. Figure 18 shows the operating points of the engine in offline and HIL simulations. The HIL simulation results are generally consistent with the offline simulation results, and only minimal deviations occur due to signal accuracy and online transmission speed.

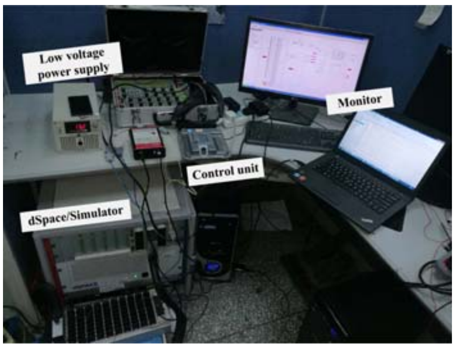

Figure 15. HIL experiment bench.

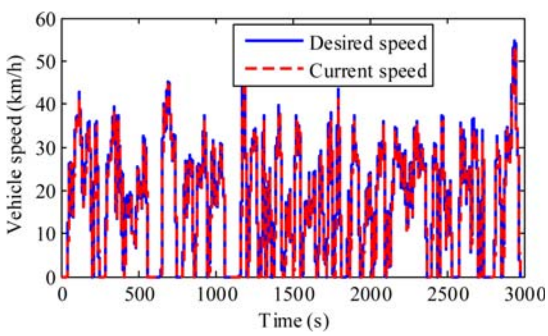

Figure 16. Vehicle speed in HIL simulation.

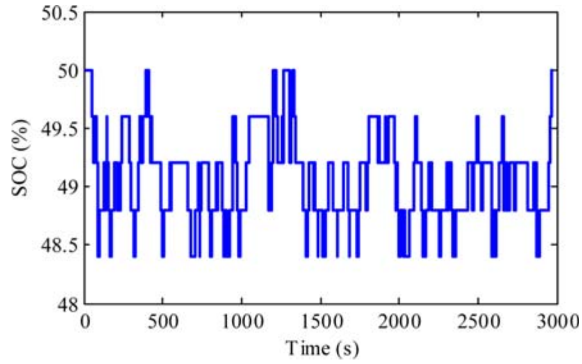

Figure 17. SOC in HIL simulation.

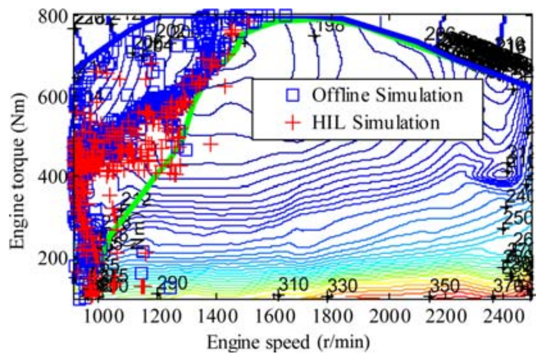

Figure 18. Comparison of engine operating points under two platforms.

6. CONCLUSION

This study proposes an online optimal control strategy methodology for power-split HEB based on historical data. Cluster analysis and Markov chain method are applied to synthesize driving cycles, which can reduce the pressure on data processing. The results show that the synthesized cycle can well represent the real operating characteristics of specific application scenarios. The DP algorithm is selected for offline global optimization to minimize the overall fuel consumption.

A novel control rule extraction method is implemented to extract the control rule from the DP solution. The extracted information is then combined with OOL-RCS to form DP-RCS. The method has a general application form, which is conducive to the understanding of engineers and application of optimal control rules. Finally, the DP-RCS is compared with DP algorithm and OOL-RCS. The results show that DP-RCS based on synthesized cycle can obtain the approximate optimal control effect to DP results, with fuel saving of 7 %. The HIL simulation test shows that the proposed online optimal control strategy has good real-time performance.

In conclusion, the online optimal control strategy methodology proposed in this work provides a reference for solving the calibration problem for power-split HEBs, which give full play to the fuel-saving potential in various driving cycles. Moreover, the proposed methodology is an important part of the future big data computing platform, which creates possibilities for online automatic optimization and calibration of control strategies.

ACKNOWLEDGEMENT−This study was financially supported by key research and development plan of China (2018YFB0105900).

REFERENCES

Awadallah, M., Tawadros, P., Walker, P. and Zhang, N. (2017). Dynamic modelling and simulation of a manual transmission based mild hybrid vehicle. *Mechanism and Machine Theory*, **112**, 218−239.

Biasini, R., Onori, S. and Rizzoni, G. (2013). A near-optimal rule-based energy management strategy for medium duty hybrid truck. *Int. J. Powertrains*, **2**, **2-3**, 232−261.

Borthakur, S. and Subramanian, S. C. (2018). Optimized design and analysis of a series-parallel hybrid electric vehicle powertrain for a heavy duty truck. *IFAC-PapersOnLine* **51**, **1**, 184−189.

Chen, L., Geng, C. L. and Song, J. J. (2017). Modeling and simulation of a novel HEV automatic transmission system for heavy duty vehicles. *IEEE. 29th Chinese Control and Decision Conf.*, 1368−1372.

Dong, B., Tian, Y. T. and Zhou, C. J. (2014). Energy management system optimal strategy for pure electric vehicle based on the dynamic programming. *Applied Mechanics and Materials*, **556-562**, 1472−1475.

Duan, B. M., Wang, Q. N., Zeng, X. H., Gong, Y. S., Song, D. F. and Wang, J. N. (2017). Calibration methodology for energy management system of a plug-in hybrid electric vehicle. *Energy Conversion and Management*, **136**, 240−248.

Fu, J. T., Song, S. Z., Fu, Z. M. and Ma, J. W. (2017). Real-time implementation of optimal control considering gear shifting and engine starting for parallel hybrid electric vehicle based on dynamic programming. *Optimal Control Applications and Methods* **39**, **2**, 757−773.

Gavgani, A. M., Sorniotti, A., Doherty, J. and Cavallino, C. (2016). Optimal gearshift control for a novel hybrid electric drivetrain. *Mechanism and Machine Theory*, **105**, 352−368.

Gujarathi, P. K., Shah, V. and Lokhande, M. (2017). Performance analysis of converted parallel plug-in hybrid electric vehicle. *IEEE 8th Control and System Graduate Research Colloquium*, 191−196.

Huertas, J. I., Díaz, J., Cordero, D. and Cedillo, K. (2018). A new methodology to determine typical driving cycles for the design of vehicles power trains. *Int. J. Interactive Design and Manufacturing* **12**, **1**, 319−326.

Kum, D., Peng, H. and Bucknor, N. K. (2011). Supervisory control of parallel hybrid electric vehicles for fuel and emission reduction. *J. Dynamic Systems Measurement and Control* **133**, **6**.

Lee, T. K., Adornato, B. and Filipi, Z. S. (2011). Synthesis of real-world driving cycles and their use for estimating PHEV energy consumption and charging opportunities: case study for Midwest/U.S. *IEEE Trans.Vehicular Technology*, **60**, **9**, 4153−4163.

Mangun, F., Idres, M. and Abdullah, K. (2017). Design optimization of a hybrid electric vehicle powertrain. *Int. Conf. Materials Science and Engineering*, **184**.

Peng, J. K., He, H. W. and Xiong, R. (2016). Rule based energy management strategy for a series–parallel plug-in hybrid electric bus optimized by dynamic programming. *Applied Energy*, **185**, 1633−1643.

Peng, Y. H., Yuan, Z. and Yang, H. B. (2019). Development of a representative driving cycle for urban buses based on the K-means cluster method. *Cluster Computing*, **22**, **3**, 6871−6880.

Qi, Y. L., Xiang, C. L., Wang, W. D., Wen, B. X. and Ding, F. (2018). Model predictive coordinated control for dual-mode power-split hybrid electric vehicle. *Int. J. Automotive Technology* **19**, **2**, 345−358.

Shahidinejad, S., Bibeau, E. and Filizadeh, S. (2010). Statistical development of a duty cycle for plug-in vehicles in a North American urban setting using fleet information. *IEEE Trans. Vehicular Technology*, **59**, **8**, 3710−3719.

Wang, S. L., Lin, B., Zhang, X. F., Liang, J. M. and Wang, Y. (2015). A novel tool path generation algorithm for plane envelope grinding convex surface based on constant scallop height method. *Int. J. Advanced Manufacturing Technology*, **78**, **5-8**, 1087−1099.

Wang, W. H., Song, R. F., Guo, M. C. and Liu, S. S. (2014). Analysis on compound-split configuration of power-split hybrid electric vehicle. *Mechanism and Machine Theory*, **78**, 272−288.

Xi, L. H., Zhang, X. and Sun, C. (2016). Energy management strategy for E-REV based on dynamic programming. *J. Beijing Jiaotong University*, **40**, **5**, 120−125.

Xi, L. H., Zhang, X., Geng, C. and Xue, Q. C. (2018). Energy management strategy optimization of extended-range electric vehicle based on dynamic programming. *J. Traffic and Transportation Engineering*, **18**, **3**, 148−

156.

Yang, S. C., Gu, Y. and Li, M. (2014). Offline optimization of parallel hybrid electric vehicle energy management strategy based on the dynamic programming. *Advanced Materials Research*, **1044-1045**, 941–946.

Zeng, X. H., Yang, N. N., Song, D. F., Zhang, C., Wang, J. N., Wang, J. X. and Wang, Q. N. (2016). Multi-factor integrated parametric design of power-split hybrid electric bus. *J. Cleaner Production*, **115**, 88-100.

Zhang, Y. H., Jiao, X. H., Li, L., Yang, C., Zhang, L. P. and Song, J. (2014). A hybrid dynamic programming-rule based algorithm for real-time energy optimization of plug-in hybrid electric bus. *Science China Technological Sciences*, **57**, **12**, 2542–2550.

Zhao, J. Y., Gao, Y. H., Guo, J. H. and Chu, L. (2018). The creation of a representative driving cycle based on Intelligent Transportation System (ITS) and a mathematically statistical algorithm: a case study of changchun (China). *Sustainable Cities and Society*, **42**, 301–313.